

## Title

*On the drivers of phytoplankton blooms in the Antarctic marginal ice zone: a modeling approach*

## Authors

Marc H. Taylor<sup>1\*</sup>, Martin Losch<sup>1</sup>, and Astrid Bracher<sup>1,2</sup>

## Author Affiliations

<sup>1</sup> Alfred Wegener Institute for Polar and Marine Research, PO Box 120161, D-27515 Bremerhaven, Germany

<sup>2</sup> Institute of Environmental Physics, University of Bremen, PO Box 330440, D-28334 Bremen, Germany

\* Corresponding author: [marchtaylor@yahoo.com](mailto:marchtaylor@yahoo.com)

## Abstract

The pelagic province of the Southern Ocean generally has low levels of primary production attributable to a short growing season in the higher latitudes, a deep mixed layer, and iron limitation. Exceptions include phytoplankton blooms in the marginal ice zone (MIZ) during spring and summer sea ice retreat. The prevailing hypothesis as to the drivers of the blooms is that sea ice retreat increases the vertical stability of the water column through the production of melt water and provides shelter from wind-mixing in areas of partial sea ice coverage. These conditions are favorable to phytoplankton growth by allowing them to maintain their

position in the upper reaches of the water column. This work investigates the drivers MIZ blooms using a biochemically-coupled global circulation model. Results support the hypothesis in that physical conditions related to a shallow, vertically stable water column (e.g. mixed layer depth and available light) were the most significant predictors of bloom dynamics, while nutrient limitation was of lesser importance. We estimate that MIZ blooms account for 15% of yearly net primary production in the Southern Ocean and that the earlier phases of the MIZ bloom, occurring under partial ice coverage and invisible to remote sensing, account for about two-thirds of this production. MIZ blooms were not found to enhance depth-integrated net primary production when compared to similar ecological provinces outside of the MIZ, although the elevated phytoplankton concentrations in surface waters are hypothesized to provide important feeding habitats for grazing organisms, such as krill.

## **Keywords**

Physical - Biological Coupling; Phytoplankton dynamics; Marginal ice zone; Phytoplankton bloom; Southern Ocean

## **1. Introduction**

### **1.1. Seasonal Ice Zone Biochemical Province**

The seasonal ice zone (SIZ) extends hundreds of kilometers from the Antarctic coast [Sakshaug *et al.*, 1991] with sea ice typically being less than 1 m thick [Pfaffling *et al.*, 2007] and growing from April and melting from October. The offshore water masses are characterized by latitudinal gradients in nutrients during the winter, which reflect the

circumpolar frontal structure [Dafner *et al.*, 2003]. The major fronts are found at 40°S (sub-tropical front), 45°S (sub-Antarctic front), 50°S (Antarctic polar front), and ca. 52° to > 60°S the southern boundary of the Antarctic Circumpolar Current (ACC) [Orsi *et al.*, 1995]. Treguer and Jacques [1992] estimated the SIZ area at  $16 \times 10^6 \text{ km}^2$ , making it the largest of the Southern Ocean biogeochemical provinces identified in their review. The SIZ extends annually as far north as 55°S, while the southernmost areas of the SIZ lie directly over the Antarctic shelf, in the physical domain of the counter-clockwise Coastal Current.

The Southern Ocean has been described as the largest high-nutrient low-chlorophyll (HNLC) region in the world ocean [Martin *et al.*, 1990; Minas and Minas, 1992]. Low levels of primary production have been attributed to the relatively short growing season in the higher latitudes, a deep mixed layer, and iron limitation [Martin *et al.*, 1990; Mitchell and Holm-Hansen, 1991; Boyd *et al.*, 2000]. It is hypothesized that, for open ocean areas of the SO, phytoplankton growth rates are enhanced by oceanographic fronts, whereby divergence of surface waters can bring iron-replete waters into the euphotic zone [Hense *et al.*, 2000; Moore and Abbott, 2000; Osmund Holm-Hansen and Hewes, 2004; O. Holm-Hansen *et al.*, 2005; Sokolov and Rintoul, 2007]. In open water, the timing and intensity of the spring bloom varies greatly, probably on account of water mass interactions [Dafner *et al.*, 2003].

The highest levels of Southern Ocean primary production have been associated with coastal polynyas [Arrigo and van Dijken, 2003; 2007], marginal ice zone (MIZ) blooms [Smith and Nelson, 1985; 1986], and the continental shelf [Smith and Gordon, 1997; Arrigo and van Dijken, 2004]. Again, iron supply has been suggested to be a factor, with important sources being the interaction between the ACC and bottom topography, upwelling, vertical diffusion and melting of ice and icebergs (Moore *et al.*, 1999; Fung *et al.*, 2000; Law *et al.*, 2002; Holm-Hansen *et al.*, 2005).

70

## 71 **1.2. Drivers of Marginal Ice Zone Blooms**

72         Of interest to this study are MIZ blooms occurring in the more pelagic extensions of  
73 the SIZ. From a physical standpoint, the MIZ is has been defined as "that part of the ice cover  
74 which is close enough to the open ocean boundary to be affected by its presence" [*Wadhams*  
75 *et al.*, 1986]. In the context of associated phytoplankton blooms, a more bio-centric definition  
76 is usually applied to water characteristics; specifically, areas displaying vertical stability due  
77 to the production of meltwater during the seasonal ice retreat [*Sullivan et al.*, 1988]. Although  
78 this includes conditions of partial ice coverage, remote sensing studies are restricted to open  
79 water, and thus usually define the MIZ based on the recency of sea ice presence as a proxy for  
80 stratification and/or nutrient input.

81         It is hypothesized that the stabilization of the surface layer by ice melt during the  
82 spring provides perfect growth conditions for phytoplankton by allowing for their  
83 concentration in the upper reaches of the euphotic zone [*Smith and Nelson*, 1985]. In concert  
84 with conditions of ice melt is the increased availability of light to the water column, which is  
85 ultimately needed for photosynthesis. *Smith and Comiso* [2008] find that the influence of the  
86 ice cover varies regionally and that only when the ice cover is thick and closed does it tend to  
87 control the light availability and hence the initiation of the bloom.

88         The duration of the bloom also depends upon nutrient availability and the maintenance  
89 of vertical stability, which is reflected by a shallow mixed layer. Vertical stability is likely to  
90 be disrupted once protection from partial sea ice coverage has diminished and surface waters  
91 are subjected to wind mixing. Support for this scenario comes from remote sensing  
92 observations indicating that bloom occurrence and intensity in the MIZ is correlated with  
93 wind speeds [*Fitch and Moore*, 2007]. Specifically, wind speeds above 5 m·s<sup>-1</sup> were

negatively correlated with surface chlorophyll whereas below 5 m·s<sup>-1</sup> were positively correlated.

Diatoms dominate in highly stratified waters of the MIZ, whereas *Phaeocystis antarctica* assemblages dominate where waters are more deeply mixed [Arrigo *et al.*, 1999; Goffart *et al.*, 2000]. The question of whether algae released from melting ice seed the pelagic spring phytoplankton bloom has been under debate for many years [e.g. Lancelot *et al.*, 1993]. Phytoplankton populations observed within sea ice, themselves seeded from the pelagic population as phytoplankton are incorporated into the ice growth, have been found during some studies to resemble closely the pelagic populations in spring as well as in autumn [Krell *et al.*, 2005], while other studies observe different communities as compared to the pelagic population [Mathot *et al.*, 1991]. There are three possible scenarios for the origins of the spring MIZ bloom: a) the sympagic population seeds the spring pelagic bloom upon ice melt, or b) a background ‘ambient’ population of cells which survives the winter beneath the sea-ice (perhaps as cysts) seeds the spring pelagic bloom once conditions improve, or c) cells to the north of the ice-edge proceed southwards with the retreating sea-ice. Each of these scenarios is supported by documentation of the survival strategies of Antarctic phytoplankton.

### 1.3. Modeling Approach

MIZ blooms have been reported on numerous occasions from both *in situ* data [Smith and Nelson, 1985; 1990; Lancelot *et al.*, 1993; Bracher *et al.*, 1999; Buesseler *et al.*, 2003] and from remotely sensed data [Moore and Abbott, 2000; Fitch and Moore, 2007; Arrigo *et al.*, 2008; Smith and Comiso, 2008]. MIZ blooms have been suggested to contribute a significant portion to overall Southern Ocean primary production due to the widespread occurrence of MIZ conditions during seasonal ice retreat. Smith and Nelson [1986] estimated

that overall pelagic primary productivity for the entire Southern Ocean would be increased by at least 60% if ice edge production were considered. However, recent remote sensing estimates by Arrigo et al. [2008] show that MIZ zones contribute 4.4% of total Southern Ocean primary production and do not substantially increase productivity over non-MIZ conditions. Nevertheless, these estimates are likely to be conservative because the presence of sea ice prevents estimates of ocean color via remote sensing (Fig. 1), even within the ice-edge or low ice concentrations [Belanger et al., 2007]. It has been suggested that this is a likely source of underestimation in remote estimates given that areas of partial ice coverage may receive a substantial amount of irradiance into the water column to drive primary production [Smith and Comiso, 2008].

The tradeoff between localized *in situ* sampling, which is limited to shipboard sampling, and remote sensing estimates, which offers an incomplete view during MIZ conditions, illustrates the difficulty in the investigation of blooms. As an alternative, numerical ocean modeling allows for the examination of MIZ blooms over large areas and over the full growth period. In addition, modeling can help to elucidate the drivers behind MIZ blooms by allowing for the investigation of a range of parameters relating to phytoplankton dynamics.

The objectives of this work focus on two main aspects of the MIZ: 1) To assess the drivers of MIZ blooms within the modeled ecosystem using a multivariate statistical approach and 2) Characterize the importance of MIZ blooms to overall Southern Ocean primary production. Finally, we discuss the possible implications of MIZ bloom dynamics for the lifecycle of the trophically-important krill.

## 2. Methods

### 2.1. Description of the Bio-Physically Coupled Global Circulation Model

Simulations were conducted using the Massachusetts Institute of Technology General Circulation Model (MITgcm) [Marshall *et al.*, 1997; MITgcm Group, 2012], which is integrated on a cubed-sphere grid, permitting relatively even grid spacing while avoiding polar singularities [Adcroft *et al.*, 2004]. Each face of the cube is comprised of a 510×510 grid (mean spacing = 18 km) and 50 vertical levels ranging in thickness from 10 m near the surface to approximately 450 m at a maximum model depth of 6150 m [Menemenlis *et al.*, 2008]. Initial conditions, spin-up, physical forcing fields, sea ice and further details of the global model are described in Section 3 of Losch *et al.* [2010]. Of particular relevance to phytoplankton growth in the SIZ is the parameterization of light transmission through sea ice and into the euphotic zone; details on the parameterization of these processes can be found in the Appendix. The simulation spanned the years 1992 through 2007.

The MITgcm was coupled with a version of the biogeochemical model REcoM ("Regulated Ecosystem Model") [Schartau *et al.*, 2007]. REcoM uses phytoplankton growth parameterizations of Geider *et al.* [1998] in order to account for the effect of varying stoichiometry on phytoplankton growth and, subsequently, nutrient cycling and other biological processes. Loss of phytoplankton biomass is assumed to be due to grazing, particle aggregation, exudation, and leakage. Additional parameterization has been added to account for silica and iron limitation of phytoplankton growth [Hohn, 2009]. In this form, the phytoplankton component of the model mainly describes dynamics associated with a diatom dominated community. For additional details see Losch *et al.* [submitted].

Initial condition of all REcoM variables are derived from a spun-up simulation with a coarse version of the model [based on Hohn, 2009] by interpolation onto the fine grid. The

first year (1992) of the coupled high-resolution run is not used in the analysis. With the initial conditions from the coarse resolution the model, simulated nutrient distributions are non-limiting for nitrogen in the SO, non-limiting for silica south of 45°S and limiting for iron in the 40°S-60°S latitude band. Further south the surface is frequently replenished with iron from deeper layers via vertical mixing during ice formation and iron is only marginally limiting [see also *Hohn*, 2009, Fig. 4.12]. Additional details regarding iron chemistry and the initial conditions for iron concentration can be found in the Appendix.

## 2.2. Selection of Focus Areas

The performance of the simulation was assessed through a comparison to remotely-sensed data. Daily means from remotely sensed sea ice coverage, sea surface temperature and chlorophyll *a* were used for the comparison:

Sea ice coverage – 12.5 km resolution gridded product from IFREMER (<http://cersat.ifremer.fr/>), spanning the years 1993-2007. The product uses the ARTIST algorithm [*Spreen et al.*, 2005; *Spreen et al.*, 2008] on Special Sensor Microwave Imager (SSM/I) data [*Cavalieri et al.*, 2011].

Chlorophyll *a* – 4.62 km resolution gridded product from the GlobColour Project (<http://www.globcolour.info/>), spanning the years 1997-2007. We used the GSM merged product (Garver, Siegel, Maritorena Model) [*Garver and Siegel*, 1997; *Maritorena et al.*, 2002], which combines MERIS, MODIS, and SeaWiFS data. Due to the differences in satellite operation time, the period from 1997-2002 consists of SeaWiFS data only while 2003-onwards uses data from all three satellites.



Sea surface temperature – 4 km resolution gridded product uses AVHRR Pathfinder Version 5 data, obtained from the US National Oceanographic Data Center and GHR SST (<http://pathfinder.nodc.noaa.gov>) [Casey *et al.*, 2010], spanning the years 1993-2007.

No additional model tuning was done beyond the aforementioned tuning of REcoM in the previously run coarse resolution model. Generally, simulated mean monthly chlorophyll *a* concentrations (log-transformed) correlated to remote sensing data at  $R=0.62$  globally and  $R=0.23$  for the Southern Ocean. These global correlation values are higher than those presented by other coupled GCM studies [Schneider *et al.*, 2008; Doney *et al.*, 2009]. Lower correlations appear to be common for polar regions. In a review of both GCM and remote-sensing algorithm models of primary production, the Southern Ocean was found to be an area of highest divergence of estimates [Carr *et al.*, 2006]. In this work, we have chosen to focus our statistical analysis only on best performing sub-areas of the SIZ rather than specifically tune the MITgcm-REcoM model to SO conditions. The SIZ domain was first defined as the area covered by  $>15\%$  sea ice concentration during any point of the simulated period. Within the SIZ, criteria for best performing areas were based on the correlations (Spearman  $\rho$ ) of daily averages between simulated and remotely observed estimates. Areas must have a correlation of  $>0.5$  for sea surface temperature and sea ice coverage to qualify for further analysis. Additionally, chlorophyll *a* must have a correlation of  $>0.1$ , and only areas where at least  $10\%$  of daily spring-summer remote sensing estimates were considered. This final criterion limited our analysis to the more pelagic extension of the SIZ where a greater number of ice-free days allowed for a more robust comparison. All correlations must be significant at the  $p < 0.01$  level.

### 2.3. Statistical Approach

Several modeled parameters were assessed for their influence on surface phytoplankton concentrations (Table 1). These included four physical parameters (MLD, PAR, SST and SSS), three limiting nutrient parameters (DIN, DSI, DFE) and one biological parameter (ZOOC, i.e. as a proxy for grazing losses).

For each sub-area parameter field, an Empirical Orthogonal Function analysis (EOF) was performed to reduce the highly dimensional spatio-temporal data to a single dominant mode of variability. EOF was applied to covariance matrices based on the centered (mean subtracted) time series of the grids in each sub-area. By using the leading EOF mode's coefficient (i.e. "principal component"), a single temporal signal was derived for each modeled parameter.

EOF coefficients were used as covariates for our statistical model with surface chlorophyll *a* (CHLA) as the response variable. In order to reduce the influence of multicollinearity on fitted model terms, a pre-selection of predictor covariates was conducted based on their variance-inflation factor (VIF). We applied a commonly defined threshold for variable removal when  $VIF > 10$ . Furthermore, we defined the threshold for the mean VIF of included covariates as  $< 6$ . When violations occurred, an iterative process was used to remove covariates until both criteria were satisfied.

Using the R statistical package "mgcv", we applied a Generalized Additive Model (GAM) [S. N. Wood, 2004; S.N. Wood, 2006]. GAM models allow for non-linear relationships among covariates through the fitting of spline functions to model terms. Cubic regression splines were fit with the number of basis dimensions left open to a penalized fitting. Under these settings, the addition of regression spline "knots" is penalized by the associated increase in degrees of freedom. As a consequence, cases where non-linear regression splines do not improve the fitting will be fit by a simple linear regression.

Model fitting was done according to recommendations of Zuur et al. [2009]. A full model, which included all terms, was fit using "maximum likelihood" (ML) as a criteria for the estimation of smoothing parameters. Removal of terms was done in a stepwise fashion by comparing the fits of a "bigger" model, which included the term under consideration, versus a "smaller" model, where the term was dropped. Best models were assessed through the minimization of the Akaike information criterion (AIC) and significance via a likelihood ratio (L) test. The final model was refitted using "restricted maximum likelihood" (REML) as the fitting criteria. An example of a fitted GAM model applied to a single geographic point of the SIZ can be seen in Figure 2. Each predictor variable is fit with a spline function describing its effect on CHLA. For example, mixed layer depth contributes positively only when less than 45 meters. The example uses time signals with their actual units for easy interpretation. In the actual application using EOF coefficients, the signals are normalized (mean=0, sd=1) and of arbitrary sign, which does not affect the significance or shape of the fitted spline function in the model.

#### **2.4. Estimation of Primary Production in the Marginal Ice Zone**

In order to quantify the impact of MIZ conditions on depth-integrated net primary production (NPP), we followed the protocol outlined by Arrigo et al. [2008], whereby they distinguished four ecological provinces for the Southern Ocean (< 50 °S) based on depth and sea ice presence: 1) Pelagic (> 1000 m, 0% ice, and 0% ice for > 14 days), 2) Shelf (< 1000 m, 0% ice, and 0% ice for > 14 days), 3) Pelagic MIZ (> 1000 m, 0% ice, and > 0% ice at some time in the last 14 days), and 4) Shelf MIZ (< 1000 m, 0% ice, and > 0% ice at some time in the last 14 days). The MIZ threshold of 14 days is based on *in situ* measurements of low salinity water and phytoplankton bloom persistence following sea ice retreat [Smith and

Nelson, 1986; Lancelot *et al.*, 1991]. Arrigo *et al.* [2008] estimated NPP with an algorithm based on remotely sensed ocean color and other parameters, and thus were restricted to open water conditions (i.e. 0% sea ice coverage). Due to our ability to observe and quantify the simulated NPP even under conditions of sea ice coverage, we were able to define an alternative MIZ criterion that better captured the beginning of the bloom period. In the simulation, blooms usually began soon after the initial breakup and retreat of sea ice, when concentrations fell below 90% coverage (Fig. 3). As a consequence, the spatial development of the bloom largely follows the southward retreat of sea ice. Therefore, we also compare NPP using an alternative definition for the MIZ conditions: 5) Pelagic MIZ ( $> 1000$  m,  $< 90\%$  ice, and  $> 0\%$  ice at some time in the last 14 days), and 6) Shelf MIZ ( $< 1000$  m,  $< 90\%$  ice, and  $> 0\%$  ice at some time in the last 14 days). The two MIZ definitions will later referred to as "MIZ-0" for the Arrigo *et al.* [2008] definition and "MIZ-90" for our alternate definition.

### 3. Results

#### 3.1. Correlation to Observed Estimates and Focus Area Selection

Figure 4 shows the spatial correlations of the simulation versus remote sensing data. Nine sub-areas, with longitudinal extension of  $< 30^\circ$ , were identified that passed all of the aforementioned selection criteria (Fig. 4, bottom right). Sea surface temperature and sea ice coverage were, generally, very well correlated with observed values throughout the SIZ. Areas of lower correlation occurred inshore near larger ice shelves (i.e. polynyas), which are not explicitly modeled, and, in the case of sea ice, near the more variable outer extension of the SIZ. The correlation of chlorophyll *a* was generally lower and patchier than the other two fields, although large areas of significantly positive correlations can be seen encircling the

Antarctic continent. The fulfillment of criteria for chlorophyll *a* was the most restrictive of the comparisons to remote sensing data in defining the sub-areas for further statistical analysis.

### **3.2. Statistical Exploration**

The leading EOF mode explained a large percentage of each field's variance, usually > 75% (Fig. 5). In order to reduce the impact of multi-collinearity between the model predictors, several covariates were excluded from the GAM analysis due to their VIF. ZOOC was removed from all nine sub-area models; DIN was removed from seven sub-area models; and SST, SSS and DSI were each removed from one sub-area model (Table 2).

For all sub-area models, stepwise removals of remaining terms did not improve the model and all included terms were deemed highly significant. Fitted spline functions varied in their complexity, as revealed by their associated degrees of freedom, but in no case was there an indication that linear relationships were more appropriate. The squared correlation coefficients ( $R^2$ ) were > 0.8 for all models, indicating a relatively good predictive power (Table 2). Generally, covariates associated with physical conditions were the most significant predictors of CHLA. In particular, MLD and PAR were consistently among the most significant terms. Nutrient concentrations (DIN, DSI, and DFE) were of much lower significance (Fig. 6).

### **3.3. Primary Production of the Marginal Ice Zone**

Figure 7 shows yearly cycles in area, NPP and NPP/area by ecological province. The pelagic province dominates in terms of area and NPP although the pelagic MIZ is a significant contributor to NPP from November to January, especially when using the MIZ-90 definition.

On a per area basis, shelf provinces are the most productive, with the maximum NPP values around 250 mg C m<sup>-2</sup> d<sup>-1</sup> during November and December. Both the shelf MIZ and the pelagic MIZ had NPP/area values similar to that of the pelagic province when using the MIZ-0 definition. When applying the MIZ-90 definition, the MIZ NPP/area is much lower than its respective non-MIZ province.

Figure 8 shows yearly means in area, NPP and NPP/area by ecological province as compared to Arrigo et al [2008]. Both studies show similar values in ecological province area. NPP/area estimates of Arrigo et al [2008] are consistently ~ 2x higher, which translates to higher values for total NPP by province, although the relative contributions were similar. Our MIZ-90 definition resulted in about a 5-fold increase in area and 3-fold increase in NPP over values calculated using the MIZ-0 definition. This increased the MIZ's contribution from 5% to 15% of Southern Ocean NPP.

## **4. Discussion**

### **4.1. Drivers of Marginal Ice Zone Blooms**

Our findings support the hypothesis that the stability of a shallow pycnocline, associated with melting sea ice, is most responsible for the development of phytoplankton blooms in the MIZ [Smith and Nelson, 1985; Sullivan et al., 1988]. In particular, light availability (PAR) and mixed layer depth (MLD) are the most significant predictors of surface chlorophyll *a* dynamics in explored sub-areas of the SIZ (Fig. 6). PAR is determined primarily by season and sea ice coverage in the SIZ. MLD, as determined by gradients in water density, is mainly affected by the processes of melting sea ice and mixing of the water

column by wind. From the example GAM model (Fig. 2), we can see that the contribution of PAR is largely flat after a minimum threshold is reached, and similar spline function forms were also observed in each of the sub-area models. This threshold is met once the sea ice begins to break up in spring, and it is this melting that also results in a shallow MLD due to the strong density gradient created by the fresh water lens of less dense, lower salinity waters at the surface. Additionally, the partial ice coverage hinders mixing by surface winds. The combination of these factors allows phytoplankton to maintain their position in the high light conditions of the upper layer of the water column, which results in enhanced growth and maintains bloom conditions. The termination of the bloom coincides with sea ice concentrations reducing to levels near zero, and a deepening of the MLD in response to wind-forced mixing. This mechanism has also been observed in the MIZ through remote sensing, whereby bloom occurrence was inversely related with wind speed [Fitch and Moore, 2007]. Specifically, wind speeds  $< 5 \text{ m}\cdot\text{s}^{-1}$  were most associated with bloom conditions. This speed corresponds to the threshold for turbulent mixing and a deepening of the MLD in coastal waters [Kullenberg, 1971; 1972; 1976], with higher speeds shown to be related to decreases in phytoplankton patchiness [Therriault and Platt, 1981; Demers et al., 1987]. The GAM results also indicate that SST and SSS are relatively important predictors of chlorophyll *a* dynamics for some sub-areas. These variables are closely related to the dynamics of PAR and MLD and thus their significance is likely mainly due to their association with the formation of the freshwater lens during ice retreat.

Nutrient dynamics were less important predictors of surface chlorophyll *a* dynamics. When these variables were included in the model, they were also significant, yet to a much smaller degree than the above mentioned physical parameters. The Southern Ocean is the largest high-nutrient low-chlorophyll (HNLC) region in the world ocean [Martin et al., 1990;

354 *Minas and Minas*, 1992]. Despite concentrations of macronutrients sufficient to support a  
 355 greater phytoplankton community, there is evidence that phytoplankton growth is limited by  
 356 iron and occasionally silica [*Martin et al.*, 1990; *Treguer and Jacques*, 1992; *Boyd et al.*,  
 357 2000; *Osmund Holm-Hansen and Hewes*, 2004; *O. Holm-Hansen et al.*, 2005]. This is  
 358 particularly apparent in the pelagic waters north of the SIZ, where productivity is relatively  
 359 low. The SIZ has been shown to be less limited by silica than the larger Southern Ocean  
 360 [*Sarmiento et al.*, 2007; *Hohn*, 2009] yet iron input to the upper ocean may also be limited  
 361 outside the shallower shelf regions. Iron supply to the ocean surface is dominated globally by  
 362 atmospheric deposition [*Fung et al.*, 2000; *Mahowald et al.*, 2005]. However, in the Southern  
 363 Ocean this component is small, so that interactions between the Antarctic Circumpolar  
 364 Current and bottom topography, upwelling, vertical diffusion and melting of ice and icebergs  
 365 provide comparatively important sources of iron [*Moore et al.*, 1999; *Fung et al.*, 2000; *Law*  
 366 *et al.*, 2003; *O. Holm-Hansen et al.*, 2005]. While our model does consider some of these  
 367 processes in the cycling of iron, their dynamics were not found to have as much importance to  
 368 the overall phytoplankton dynamics in the selected sub-areas of the pelagic province (Fig. 6).  
 369 *In situ* estimates of iron concentration are scarce, especially at depth, and thus our initial fields  
 370 likely include a higher degree of error than for the other limiting nutrients. Nevertheless, a  
 371 review of Southern Ocean dissolved iron measurements did not support the link between iron  
 372 cycles and uptake by phytoplankton, and suggested that other processes might be more  
 373 important drivers in its variability (e.g., recycling, exogenous inputs, and/or mixed layer  
 374 dynamics) [*Tagliabue et al.*, 2012]. The influence of iron limitation on phytoplankton  
 375 dynamics may be more pronounced in the inshore shelf areas where vertical diffusion plays a  
 376 more important role in its resuspension to the euphotic zone. Consistent with *in situ*  
 377 observations, the highest values in simulated NPP were also found within the shelf province  
 378 (Fig. 7). Uncertainty in initial iron concentrations will likely be improved in future



simulations due to the growing amount of observed data being generated in recent years (e.g. GEOTRACES program, <http://www.bodc.ac.uk/geotraces/>).

Due to constraints of our statistical approach, we were unable to assess the impact of zooplankton grazing on phytoplankton dynamics due to problems of multi-collinearity with other covariates. We believe that these losses will likely be small at the onset of the bloom, when zooplankton development is likely to lag that of the phytoplankton, but may increase later in the growing season.

#### **4.2. Importance of the Marginal Ice Zone to Southern Ocean Primary Production**

The highest rates of primary production in the Southern Ocean are generally associated with coastal polynyas [Arrigo and van Dijken, 2003; 2007], the MIZ [Smith and Nelson, 1986], and the continental shelf [Smith and Gordon, 1997; Arrigo and van Dijken, 2004] whereas the pelagic province is usually associated with lower productive waters. One exception is along the Antarctic Polar Front due to upwelling of nutrient rich waters to the euphotic zone via divergence of surface waters [Bracher et al., 1999; Hense et al., 2000; Moore and Abbott, 2000; Tremblay et al., 2002].

Both our results and more recent remote sensing estimates, which use an algorithm developed especially for the Southern Ocean [Arrigo et al., 2008], suggest that MIZ conditions in the pelagic province do not enhance NPP over non-MIZ conditions. Given that surface chlorophyll *a* levels in the MIZ are often much higher than in the open waters and clearly show bloom conditions, lower associated NPP would appear to contradict the longstanding view that MIZ blooms are one of the areas of highest primary production in the Southern Ocean [Smith and Nelson, 1986]. Arrigo et al. [2008] argued that the most likely reason for this result over larger scales of the Southern Ocean was that the conditions

necessary to create highly productive blooms are not often met. In particular, they note that conditions leading to a well-stratified mixed layer may often fail to develop or are destroyed by wind driven turbulent mixing before a phytoplankton bloom can form [Fitch and Moore, 2007]. In other words, using the criterion of recency of sea ice presence, as a proxy for the MIZ, may falsely identify locations where conditions of vertical stability have been prematurely destroyed by wind mixing. Our results suggest that blooms are much more ubiquitous and stable in conditions of partial sea ice coverage (Fig. 3), possibly due to protection from wind mixing. Furthermore, through the inclusion of this area in the MIZ-90 definition, we find that NPP/area in the MIZ is even more dramatically reduced over estimates that use the MIZ-0 definition from Arrigo *et al.* [2008] (Figs. 7 & 8), supporting the finding that MIZ blooms are not associated with enhanced NPP. Figure 9 shows the relationship between surface chlorophyll *a* and NPP throughout the Southern Ocean, indicating lowest NPP rates associated with the higher surface chlorophyll *a* levels of the MIZ. This negative relationship is also apparent in the cross sections views, where the strongest and most concentrated surface blooms are associated with the lowest NPP. To the contrary, the non-MIZ areas of the ice-free pelagic province show the more typical positive relationship between surface chlorophyll *a* and NPP. The reduced NPP rates in the MIZ are mainly due to the lower integrated PAR caused by partial sea ice coverage, although self-shading is also likely given the elevated phytoplankton concentrations in the upper levels of the water column.

Our results suggest that MIZ conditions account for about 15% of Southern Ocean NPP. In particular, our modeling approach has allowed for the quantification of the entire development of the bloom, including the earlier stages during the initial breakup and retreat of sea ice. We estimate that these earlier phases during partial ice coverage account for about

two-thirds of MIZ NPP. Without this additional component (i.e. using the MIZ-0 definition), the contribution of MIZ to total Southern Ocean NPP would be 4.7%, which is close to the estimate of 4.4% by Arrigo *et al.* [2008]. Additionally, the inclusion of partially ice covered waters allows for a much more complete view of total yearly NPP in the Southern Ocean; by using the MIZ-0 definition (i.e. open water conditions), only 88% of the total Southern Ocean NPP was accounted for within the four ecological provinces, whereas the MIZ-90 definition accounts for 99%. The inability to estimate NPP in partially ice covered areas with remote sensing has been previously highlighted as a possible source of underestimation of NPP in the Southern Ocean [Smith and Comiso, 2008], and thus our approach has helped to shed light on the importance of the MIZ to overall Southern Ocean NPP budgets.

Given that our model largely describes the dynamics of the diatom component of the phytoplankton community, the results do not fully describe all NPP in the SO. Generally, diatoms have been shown to dominate the highly stratified waters associated with the MIZ, whereas *Phaeocystis antarctica* assemblages dominate where waters are more deeply mixed [Arrigo *et al.*, 1998; Arrigo *et al.*, 1999]; however, the phytoplankton community contains many species across a spectrum of life history strategies, including within the diatoms themselves. Nevertheless, the simplification of the modeled phytoplankton should not diminish the importance of our results regarding MIZ processes, although NPP estimates of the Southern Ocean as a whole are likely incomplete and lower than reality. For example, a newer version of the REcoM model, which incorporates nanophytoplankton, estimates that this smaller fraction accounts for 40% of Southern Ocean NPP [Hauck *et al.*, submitted].

#### **4.3. Importance of Seasonal Ice Zone Blooms for the Larger Ecosystem**

Despite the finding that MIZ processes do not enhance NPP in the pelagic province, their associated blooms may still have an important role for functioning of the larger ecosystem. MIZ blooms provide a concentrated food source in the upper layers of the water column that are likely to improve the feeding efficiency of grazing organisms. Antarctic krill (*Euphausia superba*) have long been of particular interest due to their central role in the Southern Ocean food web, both as important grazers of plankton and as prey to a variety of higher predators. Krill are found in highest abundances on the shelf, but can be generally described as a pelagic species, with 87% of the total krill stock living in deep ocean water (>2000 m) [Atkinson *et al.*, 2008].

Krill distribution largely overlaps with that of the SIZ, and sea ice habitats are required during parts of its lifecycle. Whereas adult krill are known to have a more benthic feeding mode during the winter period [Kawaguchi *et al.*, 1986], krill larvae actively feed on the sea ice biota living within and below the sea ice [Daly and Macaulay, 1991]. Several studies also link sea ice extent and duration with recruitment success and abundance changes [Siegel and Loeb, 1995; Loeb *et al.*, 1997; Atkinson *et al.*, 2004], highlighting the long-term trend towards reduced krill populations in response to global warming induced reductions in sea ice extent. This scenario is most probable for the west Antarctic Peninsula region, which has shown the largest increases in temperature and subsequent reductions in sea ice.

Food availability has been identified as the most important factor in the krill's lifecycle [Siegel, 2005; Atkinson *et al.*, 2008; Meyer *et al.*, 2009; Meyer *et al.*, 2010], including several critical stages for recruitment success [Meyer, 2012]. Our results show a maximum in the MIZ province's area and NPP during spring, a period when phytoplankton blooms have been shown to be important for successful recruitment, allowing for early ovarian development, early spawning, and multiple egg batches [Quetin and Ross, 1991; Schmidt *et al.*, 2012]. MIZ

bloom dynamics may also be of particular relevance to the first larval feeding stage (Calypptopsis 1, "C1"), which reach surface waters after their developmental ascent and must find food within the first 10 days in order to survive [Ross and Quetin, 1989]. An interesting analog from the tropics is that of the Peruvian anchovy (*Engraulis ringens*), which has been found to have highest recruitment within an "optimal environmental window" of conditions conducive to the formation of phytoplankton blooms. In particular, the relationship between wind speed and recruitment is bell-shaped with a maximum near the threshold of turbulent mixing ( $5 \text{ m}\cdot\text{s}^{-1}$ ) [Cury and Roy, 1989]. The authors hypothesized that under these optimal conditions, upwelling of nutrient-rich waters can fuel phytoplankton growth without destroying the blooms through turbulent mixing. As mentioned before, the same threshold has been associated with the diminishment of blooms in the MIZ [Fitch and Moore, 2007].

Light has been hypothesized to be an important cue in the triggering of metabolic changes in krill following winter [see review by Meyer, 2012]. From an evolutionary perspective, such mechanisms would only develop if light is a consistent and accurate cue of improved feeding conditions. Our results support this view through the finding that PAR is a highly significant predictor of surface chlorophyll *a* concentrations in the SIZ. In addition, the increase in PAR following sea ice melting will be more abrupt than the more gradual seasonal increase in daylight experienced outside the SIZ, possibly providing a more obvious cue signaling increased food availability.

## 5. Conclusions

This study sheds light on the drivers of MIZ blooms and their importance to overall primary production in the Southern Ocean. Our results support the prevailing hypothesis that

MIZ blooms are driven mainly by physical processes; *i.e.* the formation of a shallow, vertically stable water column, during sea ice retreat, allows for the development and maintenance of the phytoplankton bloom in the upper reaches of the water column. Although nutrient concentrations are significantly related to phytoplankton concentrations, bloom diminishment is more related to the deepening of the mixed layer depth, following wind-mixing.

We estimate that MIZ blooms account for about 15% of total NPP in the Southern Ocean, of which two-thirds occurs under partial ice coverage. This finding indicates that remote sensing estimates may substantially underestimate their contribution. MIZ blooms occurring under partial ice coverage are not associated with enhanced NPP over comparable open ocean areas, likely due to lower light availability caused by partial sea ice coverage. Nevertheless, the high concentration of phytoplankton within the shallow upper reaches of the water column likely provides conditions of enhanced grazing for zooplankton, such as krill, in the post-winter period of enhanced productivity. The finding that light availability is a highly significant predictor of elevated surface phytoplankton concentrations, and that these blooms are ubiquitous within the partially ice covered regions of the SIZ, supports the hypothesis that krill may use light in the triggering of metabolic changes following winter in preparation for improved feeding conditions.

## **Acknowledgements**

The authors are grateful to the German Research Foundation for funding of the project (ID: LO-1143/6). AB would also like to acknowledge funding from the Helmholtz-Gemeinschaft Deutscher Forschungszentren e.V. (HGF) Innovative Fund for support of the "Phytooptics"

project. The authors thank the following people for their assistance during the study: Bank Beszteri, Tilman Dinter, Stephan Frickenhaus, Judith Hauck, Frank Kauker, Bettina Meyer, Cyril Piou, and Christoph Völker. Special thanks to Jill Schwarz for initiation of the project idea.

## A. Appendix

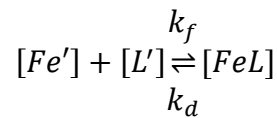
The coupled numerical biogeochemical ocean general circulation model contains many parameterizations that determine its performance in a global simulation. Here we present those parameterizations that are particularly relevant to our study: iron chemistry, iron cycling and light transmission through sea ice.

### A.1. Iron Chemistry

All biogeochemical tracers of REcoM are advected as physically passive tracers with individual local source terms. For the micronutrient iron (Fe), which limits growth via a Michaelis-Menten law with a half-saturation of  $k_{Fe} = 0.12 \mu\text{mol m}^{-3}$ , the source term consists of iron scavenging following Parekh et al. [2004], and the source term of the macronutrient dissolved inorganic carbon (DIC) scaled by a fixed iron-to-carbon ratio of 0.005. For DIC the source term consists of respiration of phytoplankton and zooplankton, a sink due to photosynthesis, degradation of extracellular organic carbon. The source term for iron then reads

$$S_A(Fe) = q^{Fe} S_A(DIC) - k_{sc} Fe'$$

with a scavenging rate  $k_{sc}$  of  $0.001 \text{ d}^{-1}$ . The free iron  $Fe'$  is computed following Parekh *et al.* [2004]



$$[Fe] = [Fe'] + [FeL]$$

$$[L_T] = [L'] + [FeL]$$

$$K_{FeL}^{cond} = \frac{[FeL]}{[Fe'][L']}$$

where  $FeL$  is complexed iron associated with an organic ligand,  $L_T$  is the total ligand, assumed constant (1),  $L'$  is free ligand, and  $K_{FeL}^{cond}$  is the conditional stability constant (100) when the system is in equilibrium.

Iron concentrations are initialized with output of the PISCES model [Aumont *et al.*, 2003]. These concentrations were determined to be too high in the Southern Ocean as compared to iron distribution fields based on *in situ* measurements by de Baar *et al.* [1999], with highest overestimation of Fe concentrations in deep waters. The PISCES data is therefore corrected towards lower concentrations in the Southern Ocean. Following this correction, the mean ( $\pm$  standard deviation) initial Fe concentrations ( $\mu\text{mol m}^{-3}$ ) of the SIZ domain were 0.022 ( $\pm 0.01$ ) at the surface and 0.326 ( $\pm 0.124$ ) at about 1000 m.

## A.2. Light transmission

The sea ice model use two “ice”-classes: open water and ice. All net fluxes, including shortwave radiation (*i.e.* light), are computed from the open water fraction and the ice fraction separately and then averaged to give the net flux. In the case of light, the net light that reaches the surface layer of the ocean model is

$$Q_{SW,net} = Q_{SW,water} * (1 - c) + Q_{SW,ice} * c$$

where  $c$  is the fractional ice cover ( $[0,1]$ ), and  $Q_{SW,ice/water/net}$  are the ice, water and net downward shortwave heat fluxes. Light can penetrate ice but is attenuated with an exponential law:

$$Q_{SW,ice} = (1 - \alpha_{ice}) Q_{SW} 0.3 * \exp(-1.5 h_{ice})$$

with the ice thickness  $h_{ice}$  measured in meters. The albedo of sea ice  $\alpha_{ice}$  is a function of temperature.  $Q_{SW}$  is the incoming shortwave radiation. In the case of a snow cover ice there is no penetration.



570

571 **References**

572 Adcroft, A., J.-M. Campin, C. N. Hill, and J. C. Marshall (2004), Implementation of an  
573 atmosphere-ocean general circulation model on the expanded spherical cube, *Mon Weather*  
574 *Rev*, 132(12), 2845-2863.

575

576 Arrigo, K. R., and G. L. van Dijken (2003), Phytoplankton dynamics within 37 Antarctic  
577 coastal polynya systems, *Journal Of Geophysical Research-Oceans*, 108(C8).

578

579 Arrigo, K. R., and G. L. van Dijken (2004), Annual cycles of sea ice and phytoplankton in  
580 Cape Bathurst polynya, southeastern Beaufort Sea, Canadian Arctic, *Geophysical Research*  
581 *Letters*, 31(8).

582

583 Arrigo, K. R., and G. L. Van Dijken (2007), Interannual variation in air-sea CO<sub>2</sub> flux in the  
584 Ross Sea, Antarctica: A model analysis, *Journal Of Geophysical Research-Oceans*, 112(C3).

585

586 Arrigo, K. R., A. M. Weiss, and W. O. Smith (1998), Physical forcing of phytoplankton  
587 dynamics in the southwestern Ross Sea, *Journal Of Geophysical Research-Oceans*, 103(C1),  
588 1007-1021.

589

590 Arrigo, K. R., G. L. van Dijken, and S. Bushinsky (2008), Primary production in the Southern  
591 Ocean, 1997-2006, *Journal Of Geophysical Research-Oceans*, 113(C8).

592

593 Arrigo, K. R., D. H. Robinson, D. L. Worthen, R. B. Dunbar, G. R. DiTullio, M. VanWoert,  
594 and M. P. Lizotte (1999), Phytoplankton community structure and the drawdown of nutrients  
595 and CO<sub>2</sub> in the Southern Ocean, *Science*, 283(5400), 365-367.

596

597 Atkinson, A., V. Siegel, E. Pakhomov, and P. Rothery (2004), Long-term decline in krill  
598 stock and increase in salps within the Southern Ocean, *Nature*, 432(7013), 100-103.

599

600 Atkinson, A., et al. (2008), Oceanic circumpolar habitats of Antarctic krill, *Marine Ecology-*  
601 *Progress Series*, 362, 1-23.

602

603 Aumont, O., E. Maier-Reimer, S. Blain, and P. Monfray (2003), An ecosystem model of the  
604 global ocean including Fe, Si, P colimitations, *Global Biogeochemical Cycles*, 17(2).

605

606 Belanger, S., J. K. Ehn, and M. Babin (2007), Impact of sea ice on the retrieval of water-  
607 leaving reflectance, chlorophyll a concentration and inherent optical properties from satellite  
608 ocean color data, *Remote Sens Environ*, 111(1), 51-68.

609

- Boyd, P. W., et al. (2000), A mesoscale phytoplankton bloom in the polar Southern Ocean stimulated by iron fertilization, *Nature*, 407(6805), 695-702.
- Bracher, A. U., B. M. A. Kroon, and M. I. Lucas (1999), Primary production, physiological state and composition of phytoplankton in the Atlantic Sector of the Southern Ocean, *Marine Ecology-Progress Series*, 190, 1-16.
- Buesseler, K. O., R. T. Barber, M. L. Dickson, M. R. Hiscock, J. K. Moore, and R. Sambrotto (2003), The effect of marginal ice-edge dynamics on production and export in the Southern Ocean along 170 degrees W, *Deep-Sea Research Part II-Topical Studies In Oceanography*, 50(3-4), 579-603.
- Carr, M. E., et al. (2006), A comparison of global estimates of marine primary production from ocean color, *Deep-Sea Research Part II-Topical Studies In Oceanography*, 53(5-7), 741-770.
- Casey, K. S., T. B. Brandon, P. Cornillon, and R. Evans (2010), The Past, Present and Future of the AVHRR Pathfinder SST Program, in *Oceanography from Space: Revisited*, edited by V. Barale, J. F. R. Gower and L. Alberotanza, Springer.
- Cavalieri, D., C. Parkinson, P. Gloersen, and Z. H. J. (2011), Sea Ice Concentrations from Nimbus-7 SMMR and DMSP SSM/I-SSMIS Passive Microwave Data, edited, National Snow and Ice Data Center, Boulder, Colorado USA.
- Cury, P., and C. Roy (1989), Optimal Environmental Window and Pelagic Fish Recruitment Success in Upwelling Areas, *Can J Fish Aquat Sci*, 46(4), 670-680.
- Dafner, E., N. Mordasova, N. Arzhanova, V. Maslennikov, Y. Mikhailovsky, I. Naletova, V. Sapozhnikov, P. Selin, and V. Zubarevich (2003), Major nutrients and dissolved oxygen as indicators of the frontal zones in the Atlantic sector of the Southern Ocean, *Journal Of Geophysical Research-Oceans*, 108(C7).
- Daly, K. L., and M. C. Macaulay (1991), Influence of Physical and Biological Mesoscale Dynamics on the Seasonal Distribution and Behavior of Euphausia-Superba in the Antarctic Marginal Ice-Zone, *Marine Ecology-Progress Series*, 79(1-2), 37-66.
- de Baar, H. J. W., J. T. M. de Jong, R. F. Nolting, K. R. Timmermans, M. A. van Leeuwe, U. Bathmann, M. R. van der Loeff, and J. Sildam (1999), Low dissolved Fe and the absence of diatom blooms in remote Pacific waters of the Southern Ocean, *Mar Chem*, 66(1-2), 1-34.
- Demers, S., J. C. Therriault, E. Bourget, and A. Bah (1987), Resuspension in the Shallow Sublittoral Zone of a Macrotidal Estuarine Environment - Wind Influence, *Limnology And Oceanography*, 32(2), 327-339.

- Doney, S. C., I. Lima, J. K. Moore, K. Lindsay, M. J. Behrenfeld, T. K. Westberry, N. Mahowald, D. M. Glover, and T. Takahashi (2009), Skill metrics for confronting global upper ocean ecosystem-biogeochemistry models against field and remote sensing data, *Journal Of Marine Systems*, 76(1-2), 95-112.
- Fitch, D. T., and J. K. Moore (2007), Wind speed influence on phytoplankton bloom dynamics in the southern ocean marginal ice zone, *Journal Of Geophysical Research-Oceans*, 112(C8).
- Fung, I. Y., S. K. Meyn, I. Tegen, S. C. Doney, J. G. John, and J. K. B. Bishop (2000), Iron supply and demand in the upper ocean, *Global Biogeochemical Cycles*, 14(1), 281-295.
- Garver, S. A., and D. A. Siegel (1997), Inherent optical property inversion of ocean color spectra and its biogeochemical interpretation .1. Time series from the Sargasso Sea, *Journal Of Geophysical Research-Oceans*, 102(C8), 18607-18625.
- Geider, R. J., H. L. MacIntyre, and T. M. Kana (1998), A dynamic regulatory model of phytoplanktonic acclimation to light, nutrients, and temperature, *Limnology And Oceanography*, 43(4), 679-694.
- Goffart, A., G. Catalano, and J. H. Hecq (2000), Factors controlling the distribution of diatoms and Phaeocystis in the Ross Sea, *Journal Of Marine Systems*, 27(1-3), 161-175.
- Hauck, J., C. Völker, T. Wang, M. Hoppema, M. Losch, and D. A. Wolf-Gladrow (submitted), Inter-annual variability of Southern Ocean organic and inorganic carbon fluxes, *Global Biogeochemical Cycles*.
- Hense, I., U. V. Bathmann, and R. Timmermann (2000), Plankton dynamics in frontal systems of the Southern Ocean, *Journal Of Marine Systems*, 27(1-3), 235-252.
- Hohn, S. (2009), Coupling and decoupling of biogeochemical cycles in marine ecosystems, 145 pp, Universität Bremen, Bremen.
- Holm-Hansen, O., and C. D. Hewes (2004), Deep chlorophyll *a* maxima (DCMs) in Antarctic waters, *Polar Biology*, 27(11), 699-710.
- Holm-Hansen, O., M. Kahru, and C. D. Hewes (2005), Deep chlorophyll *a* maxima (DCMs) in pelagic Antarctic waters. II. Relation to bathymetric features and dissolved iron concentrations, *Marine Ecology-Progress Series*, 297, 71-81.
- Kawaguchi, K., O. Matsuda, S. Ishikawa, and Y. Naito (1986), A Light Trap to Collect Krill and Other Micronektonic and Planktonic Animals under the Antarctic Coastal Fast Ice, *Polar Biology*, 6(1), 37-42.

- Krell, A., S. B. Schnack-Schiel, D. N. Thomas, G. Kattner, Z. P. Wang, and G. S. Dieckmann (2005), Phytoplankton dynamics in relation to hydrography, nutrients and zooplankton at the onset of sea ice formation in the eastern Weddell Sea (Antarctica), *Polar Biology*, 28(9), 700-713.
- Kullenberg, G. (1971), Vertical Diffusion in Shallow Waters, *Tellus*, 23(2), 129-135.
- Kullenberg, G. (1972), Apparent Horizontal Diffusion in Stratified Vertical Shear-Flow, *Tellus*, 24(1), 17-28.
- Kullenberg, G. (1976), Vertical Mixing and Energy-Transfer from Wind to Water, *Tellus*, 28(2), 159-165.
- Lancelot, C., S. Mathot, C. Veth, and H. Debaar (1993), Factors Controlling Phytoplankton Ice-Edge Blooms In The Marginal Ice-Zone Of The Northwestern Weddell Sea During Sea-Ice Retreat 1988 - Field Observations And Mathematical-Modeling, *Polar Biology*, 13(6), 377-387.
- Lancelot, C., G. Billen, C. Veth, S. Becquevort, and S. Mathot (1991), Modeling Carbon Cycling through Phytoplankton and Microbes in the Scotia-Weddell Sea Area during Sea Ice Retreat, *Mar Chem*, 35(1-4), 305-324.
- Law, C. S., E. R. Abraham, A. J. Watson, and M. I. Liddicoat (2003), Vertical eddy diffusion and nutrient supply to the surface mixed layer of the Antarctic Circumpolar Current, *Journal Of Geophysical Research-Oceans*, 108(C8).
- Loeb, V., V. Siegel, O. HolmHansen, R. Hewitt, W. Fraser, W. Trivelpiece, and S. Trivelpiece (1997), Effects of sea-ice extent and krill or salp dominance on the Antarctic food web, *Nature*, 387(6636), 897-900.
- Losch, M., D. Menemenlis, J.-M. Campin, P. Heimbach, and C. Hill (2010), On the formulation of sea-ice models. Part 1: Effects of different solver implementations and parameterizations, 33(1-2), 129.
- Losch, M., V. Strass, B. Cisewski, C. Klaas, and R. Bellerby (submitted), Ocean State Estimation from Hydrography and Velocity Observations During EIFEX with a Regional Biogeochemical Ocean Circulation Model, *Journal of Marine Systems*.
- Mahowald, N. M., A. R. Baker, G. Bergametti, N. Brooks, R. A. Duce, T. D. Jickells, N. Kubilay, J. M. Prospero, and I. Tegen (2005), Atmospheric global dust cycle and iron inputs to the ocean, *Global Biogeochemical Cycles*, 19(4).
- Maritorena, S., D. A. Siegel, and A. R. Peterson (2002), Optimization of a semianalytical ocean color model for global-scale applications, *Appl Optics*, 41(15), 2705-2714.

Marshall, J., A. Adcroft, C. Hill, L. Perelman, and C. Heisey (1997), A finite-volume, incompressible Navier Stokes model for studies of the ocean on parallel computers, *Journal Of Geophysical Research-Oceans*, 102(C3), 5753-5766.

Martin, J. H., R. M. Gordon, and S. E. Fitzwater (1990), Iron In Antarctic Waters, *Nature*, 345(6271), 156-158.

Mathot, S., S. Becquevort, and C. Lancelot (1991), Microbial Communities From The Sea Ice And Adjacent Water Column At The Time Of Ice Melting In The Northwestern Part Of The Weddell Sea, *Polar Research*, 10(1), 267-275.

Menemenlis, D., J. Campin, P. Heimbach, C. Hill, T. Lee, A. Nguyen, M. Schodlock, and H. Zhang (2008), ECCO2: High resolution global ocean and sea ice data synthesis, *Mercator Ocean Quarterly Newsletter*, 31, 13-21.

Meyer, B. (2012), The overwintering of Antarctic krill, *Euphausia superba*, from an ecophysiological perspective, *Polar Biology*, 35(1), 15-37.

Meyer, B., L. Auerswald, V. Siegel, S. Spahic, C. Pape, B. A. Fach, M. Teschke, A. L. Lopata, and V. Fuentes (2010), Seasonal variation in body composition, metabolic activity, feeding, and growth of adult krill *Euphausia superba* in the Lazarev Sea, *Marine Ecology-Progress Series*, 398, 1-18.

Meyer, B., V. Fuentes, C. Guerra, K. Schmidt, A. Atkinson, S. Spahic, B. Cisewski, U. Freier, A. Olariaga, and U. Bathmann (2009), Physiology, growth, and development of larval krill *Euphausia superba* in autumn and winter in the Lazarev Sea, Antarctica, *Limnology And Oceanography*, 54(5), 1595-1614.

Minas, H. J., and M. Minas (1992), Net Community Production in High Nutrient-Low Chlorophyll Waters of the Tropical and Antarctic Oceans - Grazing Vs Iron Hypothesis, *Oceanol Acta*, 15(2), 145-162.

Mitchell, B. G., and O. Holm-Hansen (1991), Bio-optical Properties of Antarctic Peninsula Waters - Differentiation from Temperate Ocean Models, *Deep-Sea Research Part A-Oceanographic Research Papers*, 38(8-9), 1009-1028.

MITgcm Group (2012), MITgcm Manual, Online documentation, edited, MIT/EAPS, Cambridge, MA 02139, USA.

Moore, J. K., and M. R. Abbott (2000), Phytoplankton chlorophyll distributions and primary production in the Southern Ocean, *Journal Of Geophysical Research-Oceans*, 105(C12), 28709-28722.

- Moore, J. K., M. R. Abbott, J. G. Richman, W. O. Smith, T. J. Cowles, K. H. Coale, W. D. Gardner, and R. T. Barber (1999), SeaWiFS satellite ocean color data from the Southern Ocean, *Geophysical Research Letters*, 26(10), 1465-1468.
- Orsi, A. H., T. Whitworth, and W. D. Nowlin (1995), On The Meridional Extent And Fronts Of The Antarctic Circumpolar Current, *Deep-Sea Research Part I-Oceanographic Research Papers*, 42(5), 641-673.
- Parekh, P., M. J. Follows, and E. Boyle (2004), Modeling the global ocean iron cycle, *Global Biogeochemical Cycles*, 18(1).
- Pfaffling, A., C. Haas, and J. E. Reid (2007), Direct helicopter EM - Sea-ice thickness inversion assessed with synthetic and field data, *Geophysics*, 72(4), F127-F137.
- Quetin, L. B., and R. M. Ross (1991), Behavioral and Physiological-Characteristics of the Antarctic Krill, *Euphausia-Superba*, *Am Zool*, 31(1), 49-63.
- Ross, R. M., and L. B. Quetin (1989), Energetic Cost to Develop to the 1st Feeding Stage of *Euphausia-Superba* Dana and the Effect of Delays in Food Availability, *J Exp Mar Biol Ecol*, 133(1-2), 103-127.
- Sakshaug, E., G. Johnsen, K. Andresen, and M. Vernet (1991), Modeling Of Light-Dependent Algal Photosynthesis And Growth - Experiments With The Barents Sea Diatoms *Thalassiosira-Nordenskioeldii* And *Chaetoceros-Furcellatus*, *Deep-Sea Research Part A-Oceanographic Research Papers*, 38(4), 415-430.
- Sarmiento, J. L., J. Simeon, A. Gnanadesikan, N. Gruber, R. M. Key, and R. Schlitzer (2007), Deep ocean biogeochemistry of silicic acid and nitrate, *Global Biogeochemical Cycles*, 21(1).
- Schartau, M., A. Engel, J. Schroter, S. Thoms, C. Volker, and D. Wolf-Gladrow (2007), Modelling carbon overconsumption and the formation of extracellular particulate organic carbon, *Biogeosciences*, 4(4), 433-454.
- Schmidt, K., A. Atkinson, H. J. Venables, and D. W. Pond (2012), Early spawning of Antarctic krill in the Scotia Sea is fuelled by "superfluous" feeding on non-ice associated phytoplankton blooms, *Deep-Sea Research Part II-Topical Studies In Oceanography*, 59, 159-172.
- Schneider, B., L. Bopp, M. Gehlen, J. Segschneider, T. L. Frolicher, P. Cadule, P. Friedlingstein, S. C. Doney, M. J. Behrenfeld, and F. Joos (2008), Climate-induced interannual variability of marine primary and export production in three global coupled climate carbon cycle models, *Biogeosciences*, 5(2), 597-614.

829 Siegel, V. (2005), Distribution and population dynamics of *Euphausia superba*: summary of  
830 recent findings, *Polar Biology*, 29(1), 1-22.

831

832 Siegel, V., and V. Loeb (1995), Recruitment of Antarctic Krill *Euphausia-Superba* and  
833 Possible Causes for Its Variability, *Marine Ecology-Progress Series*, 123(1-3), 45-56.

834

835 Smith, W. O., and D. M. Nelson (1985), Phytoplankton Bloom Produced by a Receding Ice  
836 Edge in the Ross Sea - Spatial Coherence with the Density Field, *Science*, 227(4683), 163-  
837 166.

838

839 Smith, W. O., and D. M. Nelson (1986), Importance Of Ice Edge Phytoplankton Production  
840 In The Southern-Ocean, *Bioscience*, 36(4), 251-257.

841

842 Smith, W. O., and D. M. Nelson (1990), Phytoplankton Growth And New Production In The  
843 Weddell Sea Marginal Ice-Zone In The Austral Spring And Autumn, *Limnology And*  
844 *Oceanography*, 35(4), 809-821.

845

846 Smith, W. O., and L. I. Gordon (1997), Hyperproductivity of the Ross Sea (Antarctica)  
847 polynya during austral spring, *Geophysical Research Letters*, 24(3), 233-236.

848

849 Smith, W. O., and J. C. Comiso (2008), Influence of sea ice on primary production in the  
850 Southern Ocean: A satellite perspective, *Journal Of Geophysical Research-Oceans*, 113(C5).

851

852 Sokolov, S., and S. R. Rintoul (2007), On the relationship between fronts of the Antarctic  
853 Circumpolar Current and surface chlorophyll concentrations in the Southern Ocean, *Journal*  
854 *Of Geophysical Research-Oceans*, 112(C7).

855

856 Spreen, G., L. Kaleschke, and D. Heygster (2005), Operational Sea Ice Remote Sensing with  
857 AMSR-E 89GHz Channels, *IEEE Internations Geoscience and Remote Sensing Symposium*,  
858 6, 4033-4036.

859

860 Spreen, G., L. Kaleschke, and G. Heygster (2008), Sea ice remote sensing using AMSR-E 89-  
861 GHz channels, *Journal Of Geophysical Research-Oceans*, 113(C2).

862

863 Sullivan, C. W., C. R. McClain, J. C. Comiso, and W. O. Smith, Jr. (1988), Phytoplankton  
864 Standing Crops Within an Antarctic Ice Edge Assessed by Satellite Remote Sensing, 93(C10),  
865 12487.

866

867 Tagliabue, A., T. Mtshali, O. Aumont, A. R. Bowie, M. B. Klunder, A. N. Roychoudhury,  
868 and S. Swart (2012), A global compilation of dissolved iron measurements: focus on  
869 distributions and processes in the Southern Ocean, *Biogeosciences*, 9(6), 2333-2349.

870

871 Therriault, J. C., and T. Platt (1981), Environmental-Control of Phytoplankton Patchiness,  
872 *Can J Fish Aquat Sci*, 38(6), 638-641.

- 873  
874 Treguer, P., and G. Jacques (1992), Dynamics Of Nutrients And Phytoplankton, And Fluxes  
875 Of Carbon, Nitrogen And Silicon In The Antarctic Ocean, *Polar Biology*, 12(2), 149-162.
- 876  
877 Tremblay, J. E., M. I. Lucas, G. Kattner, R. Pollard, V. H. Strass, U. Bathmann, and A.  
878 Bracher (2002), Significance of the Polar Frontal Zone for large-sized diatoms and new  
879 production during summer in the Atlantic sector of the Southern Ocean, *Deep-Sea Research*  
880 *Part II-Topical Studies In Oceanography*, 49(18), 3793-3811.
- 881  
882 Wadhams, P., V. A. Squire, J. A. Ewing, and R. W. Pascal (1986), The Effect of the Marginal  
883 Ice-Zone on the Directional Wave Spectrum of the Ocean, *Journal Of Physical*  
884 *Oceanography*, 16(2), 358-376.
- 885  
886 Wood, S. N. (2004), Stable and efficient multiple smoothing parameter estimation for  
887 generalized additive models, *J Am Stat Assoc*, 99(467), 673-686.
- 888  
889 Wood, S. N. (2006), *Generalized Additive Models: An Introduction with R*, Chapman and  
890 Hall/CRC.
- 891  
892 Zuur, A. F., E. N. Ieno, N. Walker, A. A. Saveliev, and G. M. Smith (2009), *Mixed effects*  
893 *models and extensions in ecology with R*, xxii, 574 p. pp., Springer, New York, NY.



898

## 899 **Figure Legends**

900 Figure 1. Fraction of days with remote estimates of chlorophyll *a* during 1997-2007  
901 (Globcolour GSM, 4 km product). Dashed line indicates the maximal extent of the SIZ

902

903 Figure 2. Example of GAM model fit to time series from a single grid location in the SIZ.  
904 Fitted smooth terms are to the right of each covariate's time series with CHLA as the response  
905 variable. Prediction values are shown as blue dots in CHLA time series.

906

907 Figure 3. Simulated daily average chlorophyll *a* concentration ( $\text{mg m}^{-3}$ ; color gradient) and  
908 sea ice coverage (%; white isolines. Two week snapshots from October 15<sup>th</sup> – December 1<sup>st</sup>,  
909 2004 (A-D) show the development of a phytoplankton bloom in areas where sea ice coverage  
910 has been reduced to below about 90 %.

911

912 Figure 4. Correlation of simulated vs. remote sensing estimates for chlorophyll *a*, sea surface  
913 temperature, and sea ice coverage. Isolines indicate areas of strong correlation among all three  
914 fields. Bottom right map shows the nine sub-areas identified for further statistical analysis.  
915 Black dashed isoline shows the maximum extent of the SIZ over the study period.

916

917 Figure 5. Variance explained by the leading EOF for each variable field.

918

Figure 6. Log likelihood ratios of GAM model term inclusion. All terms are significant at the  $p < 0.001$  level. Asterisks (\*) indicate terms not included in the sub-area model.

Figure 7. Southern Ocean ecological province yearly cycles in area (A), net primary production (NPP) (B), and net primary production per area (NPP/area) (C). Year-day mean (solid line) and standard deviation (shaded area) are shown.

Figure 8. Comparison of Southern Ocean ecological province yearly means in area (A), net primary production (NPP) (B), and net primary production per area (NPP/area) (C) to remote sensing based on estimates of Arrigo *et al.* [2008].

Figure 9. Comparison of December 2004 monthly means of surface chlorophyll *a* concentration (left) and integrated net primary production (NPP) (center). White isolines indicate the mean sea ice concentrations. Dashed black lines along 30°E and 150°W indicate the locations of the cross section views of chlorophyll *a* concentrations (right). In the cross section views, dashed white lines indicate NPP and solid white lines indicate the integrated photosynthetically active radiation (PAR) down to the depth of the mixed layer.

938

939 **Tables**

940 Table 1. Model parameter descriptions

Abbreviation	Variable	Units
CHLA	Surface chlorophyll $\alpha$	$\text{mg m}^{-3}$
MLD	Mixed layer depth	m
PAR	Integrated photosynthetically active radiation (< MLD)	$\text{W m}^{-1}$
SST	Sea surface temperature	$^{\circ}\text{C}$
SSS	Sea surface salinity	psu
DIN	Surface dissolved inorganic nitrogen	$\text{mmol m}^{-3}$
DSI	Surface dissolved silicate	$\text{mmol m}^{-3}$
DFE	Surface dissolved iron	$\mu\text{mol m}^{-3}$
ZOOC	Surface zooplankton carbon	$\text{mmol m}^{-3}$

941

942

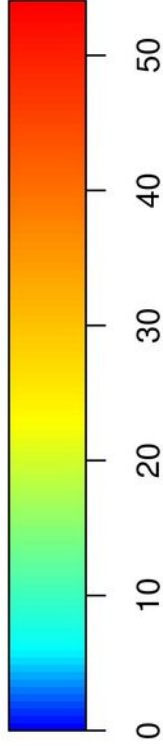
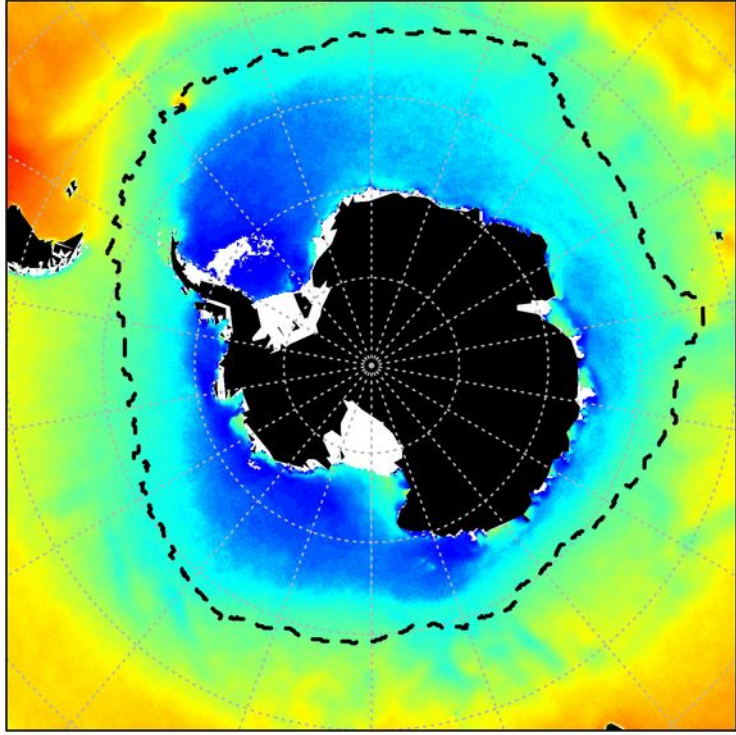
943 Table 2. Fitted GAM model statistics by SIZ area.

Area	N	R-sq. (adj.)	Terms							
			MLD	PAR	SST	SSS	DIN	DSI	DFE	
1	5478	0.83	df	7.91	7.33	8.38	8.12		8.33	8.51
			vif	4.5	2.7	4.9	6		4.5	7.1
			L*	2191	2017	907	323		140	415
2	5478	0.87	df	8.75	6.94	8.89	8.88	8.58		8.58
			vif	4.1	3.4	5.9	8.2	6		2.9
			L*	2145	2722	1326	380	176		123
3	5478	0.87	df	8.44	6.75	7.42			8.28	8.6
			vif	3.9	3.9	4.7			5.6	2.1
			L*	2581	2194	797			701	307
4	5478	0.87	df	7.8	7.35	8.01	8.55		8.56	8.77
			vif	4.9	3.9	4	8.1		6.1	3.1
			L*	1338	3965	1324	630		594	495
5	5478	0.82	df	8.08	7.09	7.06	8.18		8.46	8.7
			vif	4.7	3.3	6.3	4.9		3.4	3.4
			L*	1335	3531	424	666		213	350
6	5478	0.85	df	5.63	7.66	8.81	5.96		8.44	6.31
			vif	5.3	2.6	7.2	8.6		5.9	5.6
			L*	289	6718	1232	163		114	124
7	5478	0.83	df	7.93	8.11		8.35	8.19	8.81	8.48
			vif	3.5	1.5		3.6	7	4.3	9.2
			L*	1031	5403		72	760	395	237
8	5478	0.86	df	8.22	7.68	8.29	7.38		7.68	7.49
			vif	4.2	2.5	6.3	4.8		3.7	2.6
			L*	2566	1919	1101	904		113	365
9	5478	0.89	df	8.78	7.29	7.91	8.62		7.89	8.47
			vif	4.4	2.3	9.3	3.8		4	4.1
			L*	945	4946	2409	229		419	382

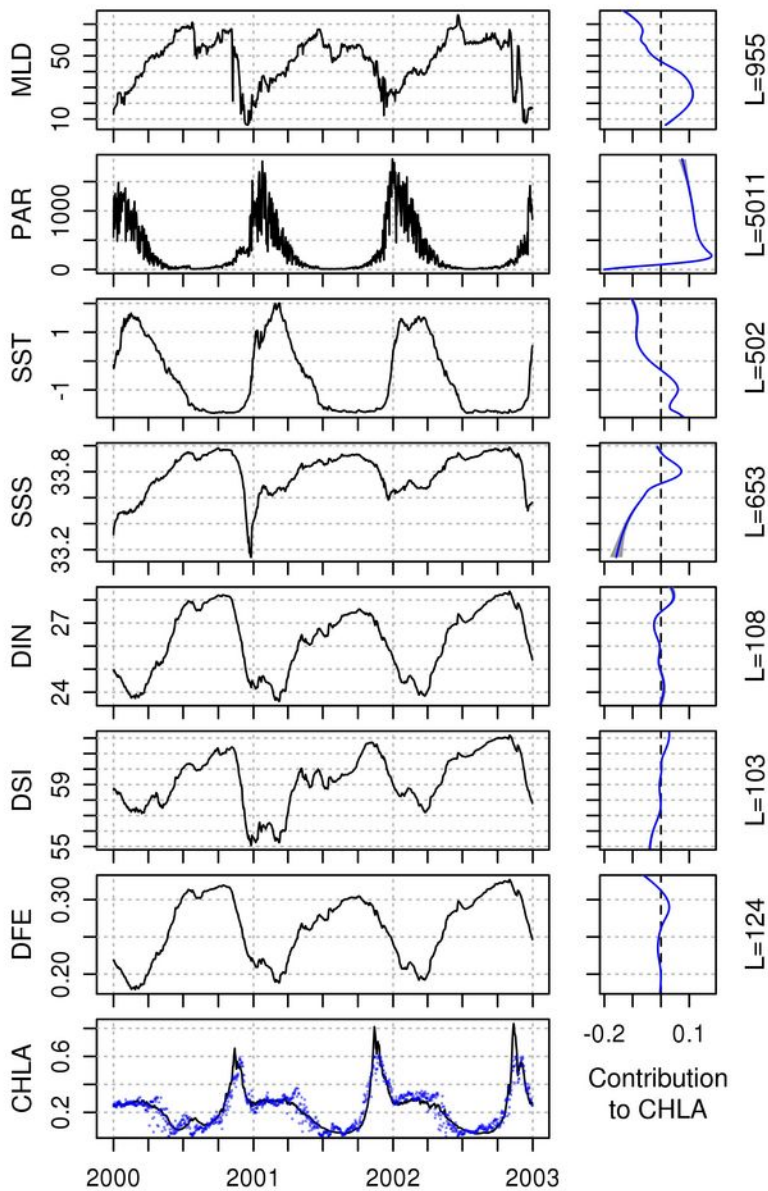
944 df = degrees of freedom, vif = variance inflation factor, L = Log likelihood ratio, (\*) All terms  
945 are significant at the p < 0.001 level

946

947

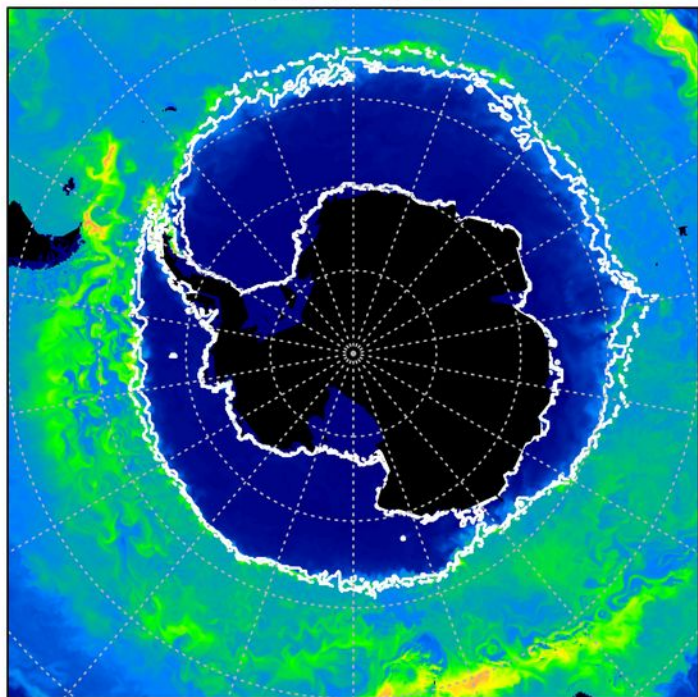


% days with remote observation

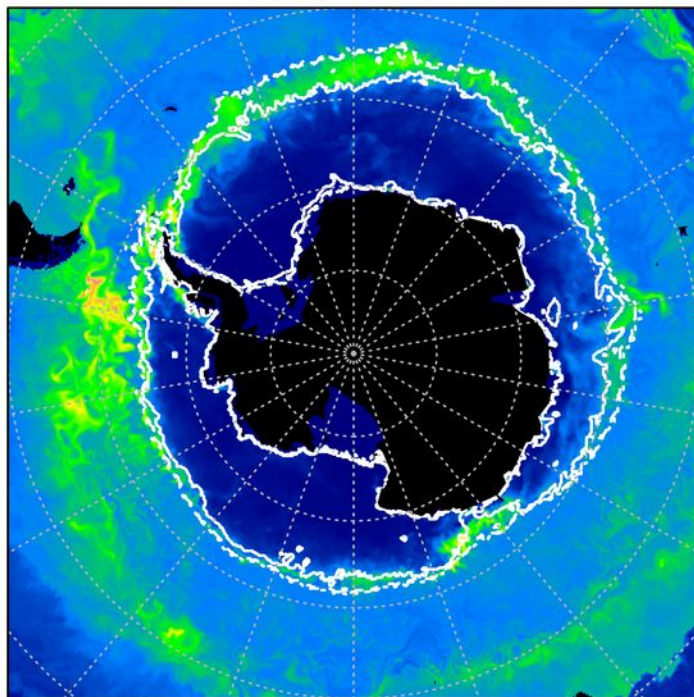




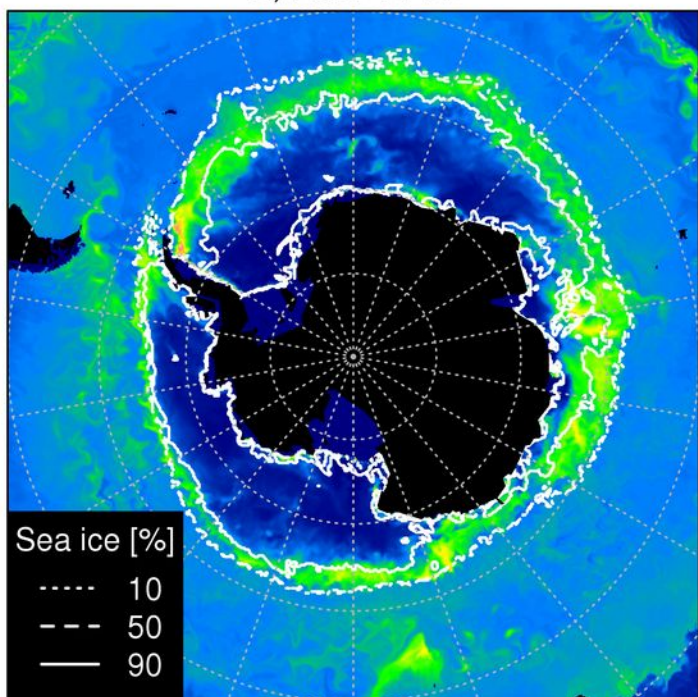
A) 2004-10-15



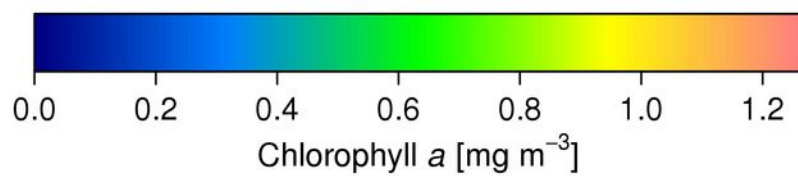
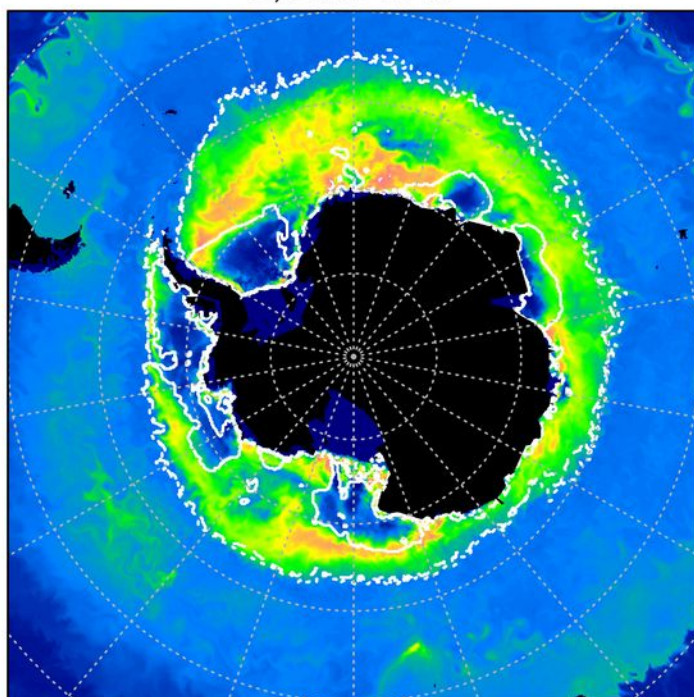
B) 2004-11-01



C) 2004-11-15

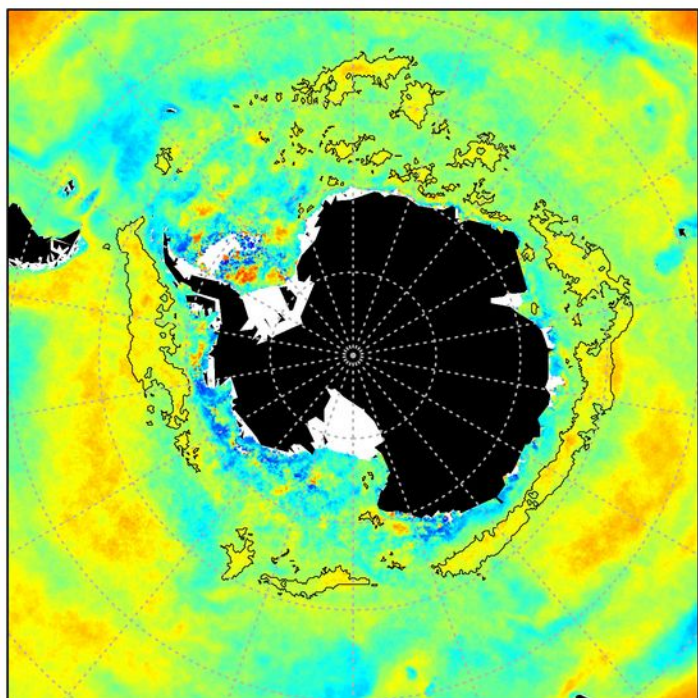


D) 2004-12-01

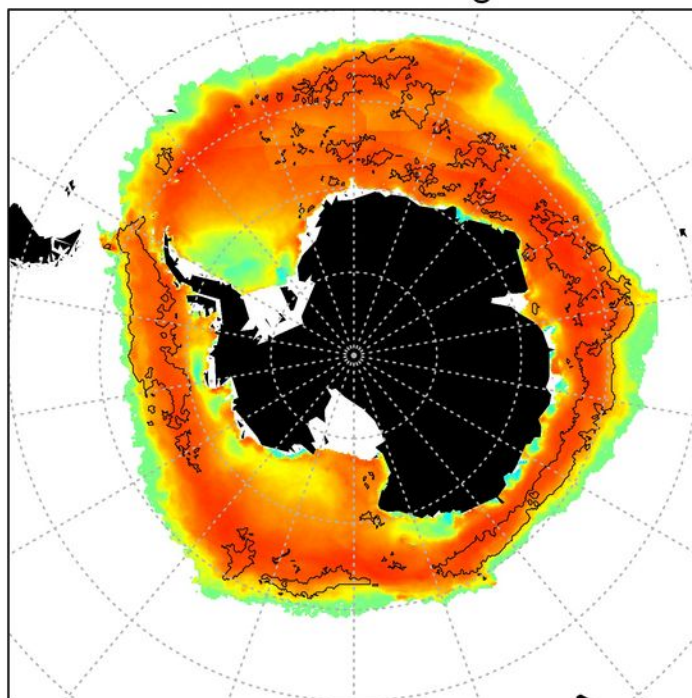




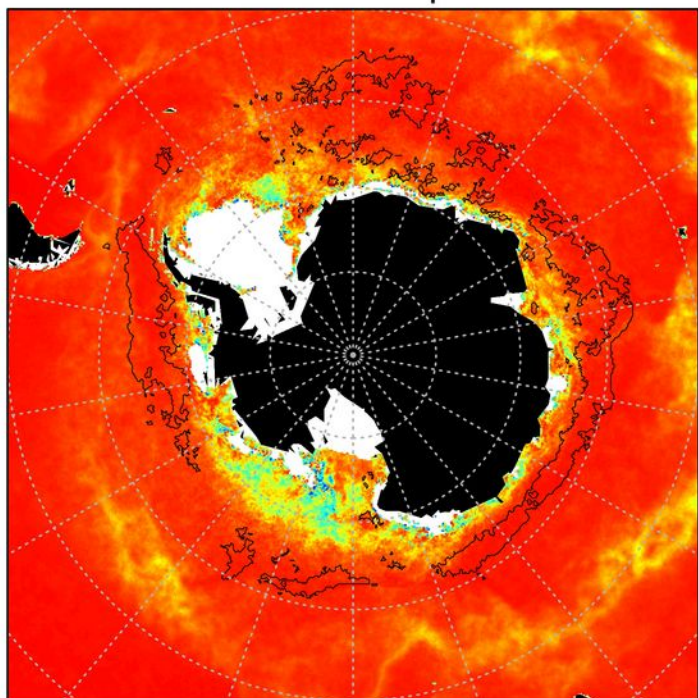
Chlorophyll *a*



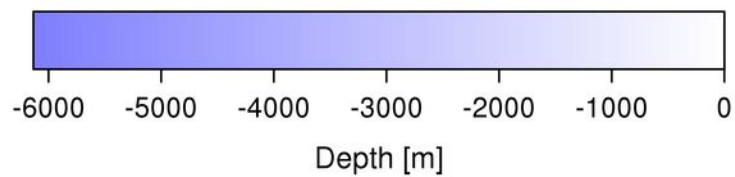
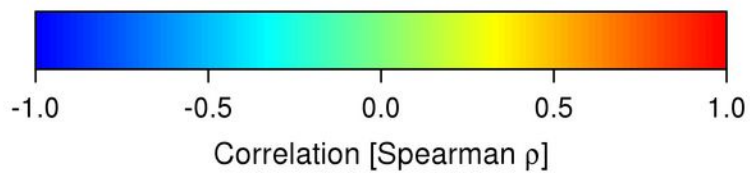
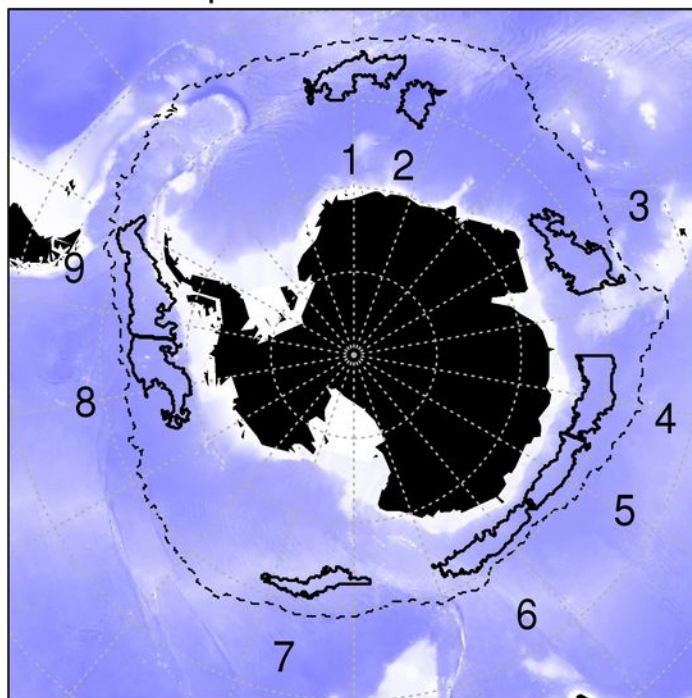
Sea ice coverage



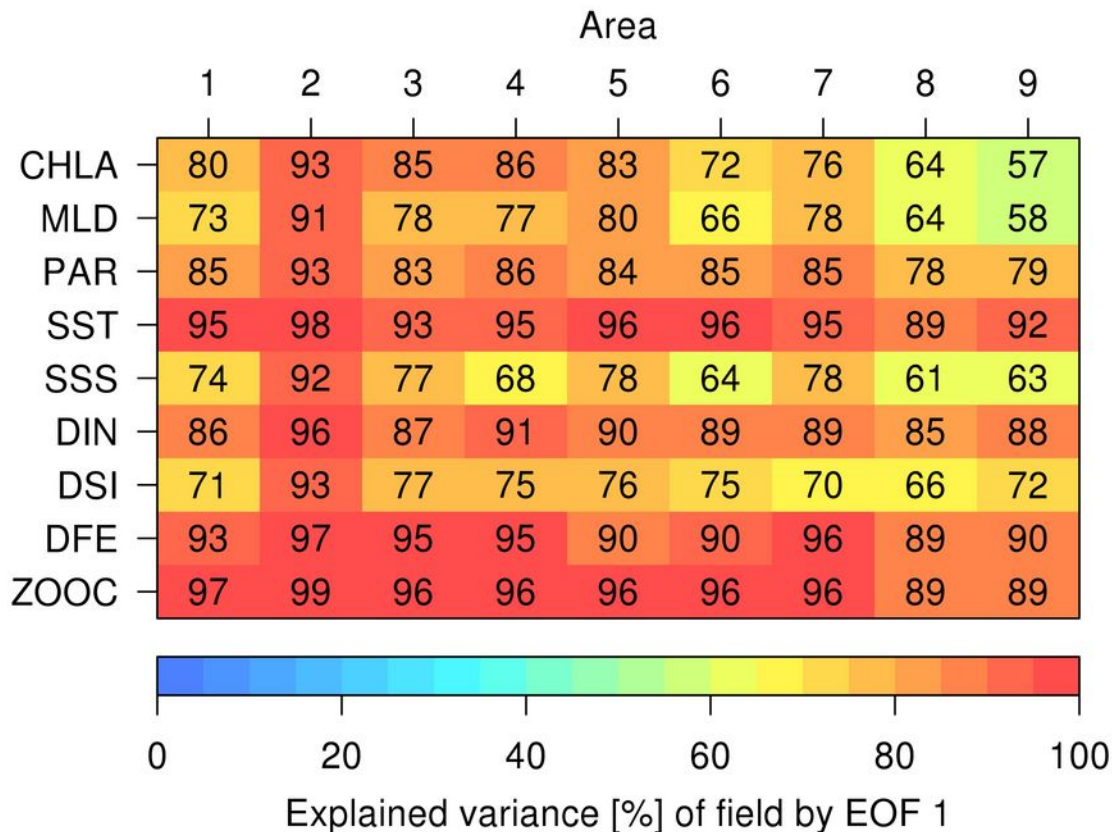
Sea surface temperature

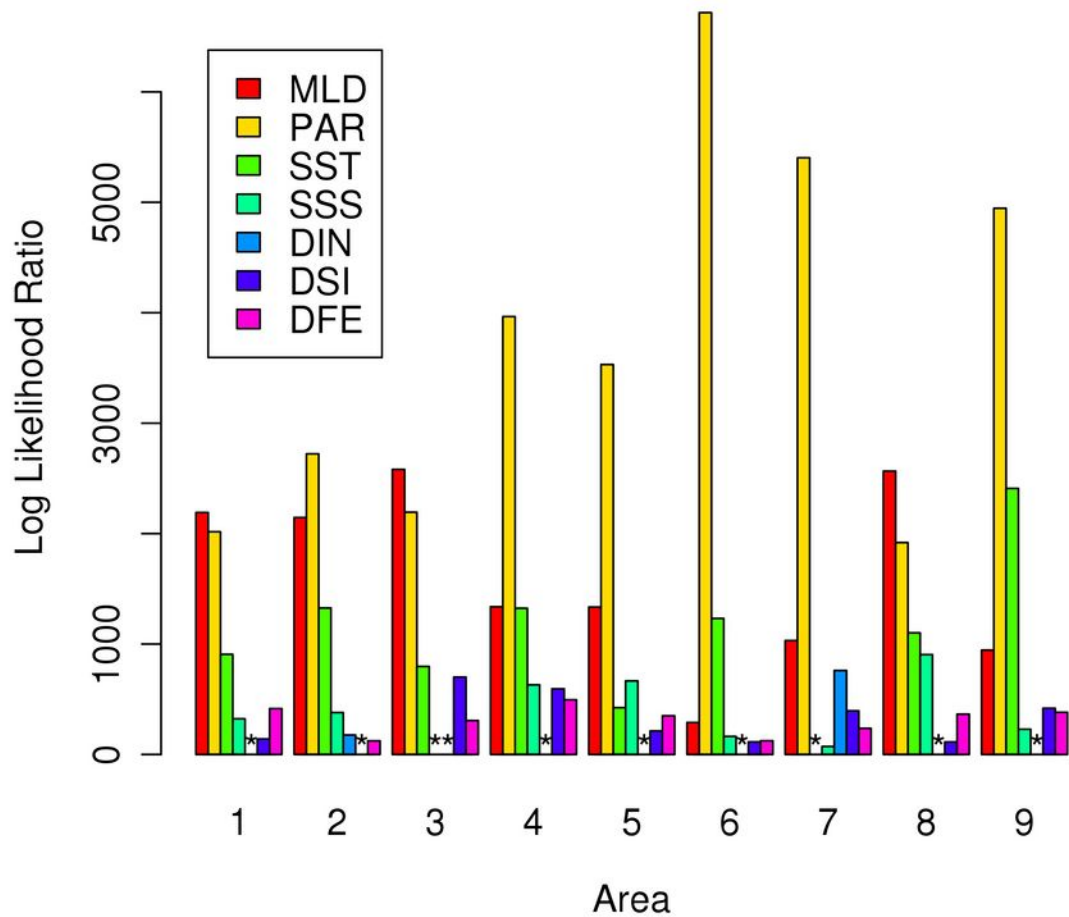


Depth with sub-areas

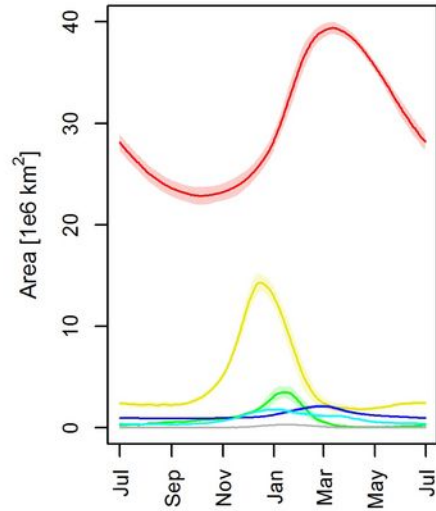




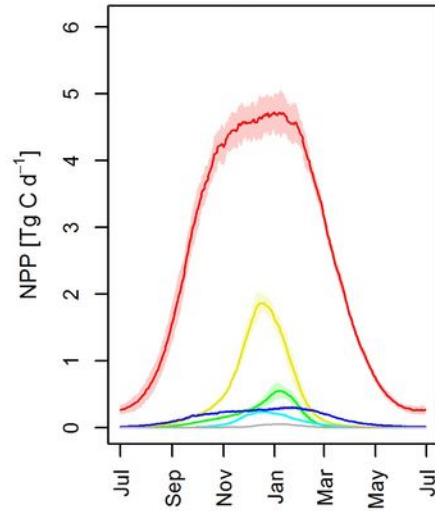




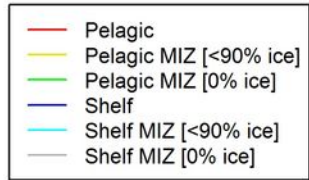
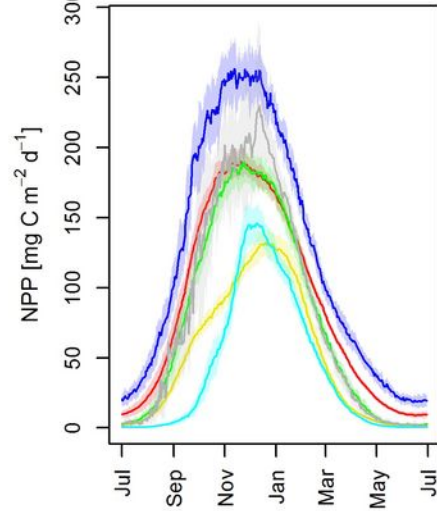
A) Area



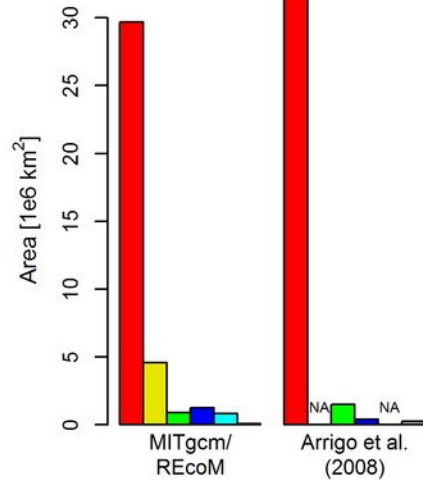
B) NPP



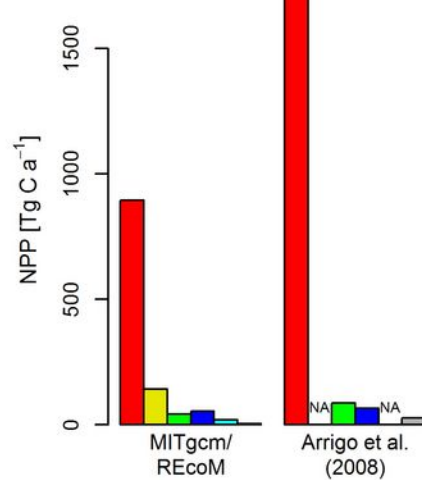
C) NPP / Area



A) Area



B) NPP



C) NPP / Area

